Atmos. Meas. Tech., 5, 1165–1172, 2012
www.atmos-meas-tech.net/5/1165/2012/
doi:10.5194/amt-5-1165-2012


Atmospheric Measurement Techniques

# DOAS-measurement of the $NO_2$ formation rate from $NO_x$ emissions into the atmosphere

**E. Frins[1], M. Osorio[1], N. Casaballe[1], G. Belsterli[1], T. Wagner[2], and U. Platt[3]**

[1]Instituto de Física, Facultad de Ingeniería, Universidad de la República, Julio Herrera y Reissig 565, Montevideo, Uruguay
[2]Max-Planck Institut für Chemie, 55128 Mainz, Germany
[3]Institut für Umweltphysik, Universität Heidelberg, Im Neuenheimer Feld 229, 69120 Heidelberg, Germany

*Correspondence to:* E. Frins (efrins@fing.edu.uy)

Received: 24 June 2011 – Published in Atmos. Meas. Tech. Discuss.: 9 September 2011
Revised: 11 April 2012 – Accepted: 28 April 2012 – Published: 24 May 2012

**Abstract.** In the present work we deal with emissions originating from combustion processes containing $SO_2$, NO and $NO_2$, emitted into the atmosphere by a localized source. We present a method for measuring the $NO_2$-formation rate (due to conversion of NO to $NO_2$) from measurements of $SO_2$- and $NO_2$-slant column densities across different plume sections, under the (usually justified) assumption that the $SO_2$-flux is constant. The advantages of the proposed method are that the measurements can be performed from an arbitrary location, without explicit reference to the wind speed and direction in the plume. We present results of ground based DOAS-measurements of $SO_2$ and $NO_x$ emissions from an oil refinery located in the northern part of Montevideo Bay and give recommendations for future applications of the method.

## 1 Introduction

Sulphur- and nitrogen-containing compounds are typical emission products from combustion processes. Their residence time in the atmosphere is affected by photochemical processes (i.e. by solar radiation), by wet and dry deposition, through interaction with aerosols as well as by chemical reactions with other species (e.g. ozone) already present in the airmass. Due to the role of nitrogen oxides in the chemistry of the atmosphere and the interplay with various cycles of other compounds, there is strong interest in having a tool for estimating their presence and time evolution together with other gases.

Remote sensing is an important tool for monitoring trace gases emitted in the atmosphere by stacks and other sources. A variety of active and passive systems (see e.g. Platt and Stutz, 2008; Bobrowski et al., 2006; Weibring et al., 2003; Louban et al., 2009; McGonigle et al., 2004; Frins et al., 2006; Kern et al., 2009 and references therein) are used for this purpose.

A widely used method to study chemical constituents of the atmosphere is the Differential Optical Absorption Spectroscopy (DOAS) (Platt and Stutz, 2008). A passive DOAS system with the sun as light source is the most simple and affordable way (McGonigle et al., 2004; Frins et al., 2006; Bobrowski and Platt, 2007; Louban et al., 2009) for monitoring the gases emitted by a localized source, e.g. a volcano or a stack. In particular $SO_2$ and $NO_2$ can be measured with passive DOAS, but not NO. The plume emitted by the source is cross-scanned through a vertical plane and the obtained absorption spectra are then analyzed using DOAS to retrieve the total slant column densities (SCDs). The data obtained at various distances from the emission source contribute to the knowledge of how the emitted gases are dispersed into the atmosphere, how they interact among themselves and with other gases, and also to achieve a better estimate of the formation rate of the gases involved in the measurement (Bobrowski et al., 2006; Hönninger, 2004; Rivera et al., 2010; Frins et al., 2011).

In order to calculate fluxes of the emitted gases, the knowledge of wind velocity in the plume is a necessary prerequisite. However, in general, the wind data (speed and direction) at the precise location of the plume is not accessible from the remote site of the measuring station. All this produces an inherent uncertainty in the determination of the

trace gases fluxes and restricts the possibility of gaining information along the path of the plume.

In the present work we will deal with emissions from combustion processes containing $SO_2$, NO, some $NO_2$ and other compounds, emitted by a stack or similar source originating from an oil refinery. Oxides of nitrogen are emitted mostly in the form of NO and some $NO_2$. NO reacts rapidly (time scale of minutes) with ozone to yield $NO_2$ (Seinfeld and Pandis, 2006), i.e.,

$$NO + O_3 \rightarrow NO_2 + O_2. \quad \text{(R1)}$$

During daytime there is a photochemical back-reaction to (R1):

$$NO_2 + h\nu \rightarrow NO + O \quad \text{(R2)}$$

where $h\nu$ denotes a photon with wavelength below 420 nm. Reaction (R1) is immediately (in the troposphere) followed by:

$$O + O_2 + M \rightarrow O_3 + M \quad \text{(R3)}$$

where $M$ denotes any air molecule. Initially and at night Reaction (R1) dominates, but in sunlight Reactions (R1)–(R3) eventually establish a photo-stationary-state ratio between $NO_2$ and NO (the well known "Leighton Ratio"). Similarly, $SO_2$ is oxidized in the gas phase, since it possesses a relatively high solubility in water, e.g. contained in clouds, fog or aerosols, also liquid-phase oxidation plays a role. However, due to the relatively low rate of these reactions (time scale of days) $SO_2$ can be considered a stable compound in comparison to NO (Lee et al., 2011).

The purpose of this paper is to present a method for measuring the formation rate of $NO_2$ (due to conversion of NO to $NO_2$) when $SO_2$ emissions are also present. Since we retrieve $NO_2$- and $SO_2$-SCD simultaneously from the same spectrum, i.e. both species are measured under the same conditions, it is possible to reference $NO_2$ against $SO_2$. Thus, by scanning the plume across different plume sections, it is possible to determine the formation rate of $NO_2$ (assuming that the total $SO_2$-flux is known and constant). The advantage of this approach relies on the fact that the measurements can be performed without explicit knowledge of the wind data at the different cross-sections of the plume.

In the next Section we describe the proposed method, and in Sects. 3 and 4 illustrative experimental results are presented and discussed.

## 2 Remote measurement of the $NO_2$ formation rate

An approach for monitoring the fluxes of trace gases emitted by a localized source and the formation rate of secondary compounds is schematically shown in Fig. 1. The technique uses a spectrometer attached to a telescope to scan the plume at different elevation angles ($\alpha_i$) and cross-sections. In Fig. 1, the dashed lines represent the directions along which the telescope is pointing, $\hat{n}$ denotes the unit vector orthogonal to the corresponding cross-section, and $\boldsymbol{v}$ is the wind velocity.

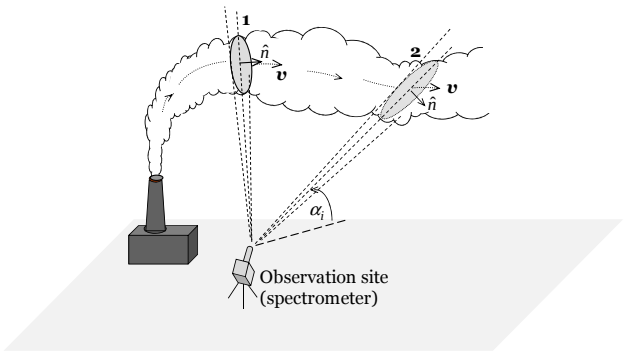


**Fig. 1.** Flux measurement across two cross-sections of a plume. The dashed lines represent the directions at elevation angle $\alpha_i$ along which the telescope is pointing, $\hat{n}$ denotes the unit vector orthogonal to the corresponding cross-section, and $\boldsymbol{v}$ is the wind velocity.

The fluxes of $NO_2$ and $SO_2$ (to be denoted as $\Phi_{NO_2}$ and $\Phi_{SO_2}$, respectively) are defined as

$$\Phi_{NO_2,SO_2} = \int_{\alpha} \int_{r} c_{NO_2,SO_2}(r,\alpha)\, \hat{n} \cdot \boldsymbol{v} r \mathrm{d}r \mathrm{d}\alpha \quad (1)$$

where $c_{NO_2,SO_2}(r,\alpha)$ are the $NO_2$- and $SO_2$-concentrations as function of the elevation angle $\alpha$(in radians), and $r$ is the distance to the plume measured from the instrument location.

Assuming that the geometrical cross section of the plume is small in comparison with the distance $R$ between observation site and plume center, and that the difference between two consecutive elevation angles is small ($\alpha_{i+1} - \alpha_i = \Delta\alpha_i \ll 1$), we can approximate Eq. (1) as

$$\begin{aligned} \Phi_{NO_2,SO_2} &= \hat{n} \cdot \boldsymbol{v}\, R \int_{\alpha} \int_{r} c_{NO_2,SO_2}(r,\alpha) \mathrm{d}r \mathrm{d}\alpha \\ &= \hat{n} \cdot \boldsymbol{v}\, R \int_{\alpha} S_{NO_2,SO_2}(\alpha) \mathrm{d}\alpha \\ &\approx \hat{n} \cdot \boldsymbol{v}\, R \sum_i S_{iNO_2,SO_2} \Delta\alpha_i \end{aligned} \quad (2)$$

where $S_{iNO_2,SO_2}$ denotes the slant column densities of $NO_2$ and $SO_2$ measured at the elevation angle $\alpha_i$, i.e.,

$$S_{iNO_2,SO_2} = \int c_{NO_2,SO_2}(r,\alpha_i) \mathrm{d}r. \quad (3)$$

As the slant column densities of $NO_2$and $SO_2$ are obtained from the same spectrum, at a given elevation angle $\alpha_i$ we will have the same values of $\hat{n} \cdot \boldsymbol{v}$ and $R$ for both species. Thus, eliminating the factor $\hat{n} \cdot \boldsymbol{v}\, R$ from Eq. (2) one easily obtains

$$\Phi_{NO_2} = \Phi_{SO_2} \frac{\sum_i S_{iNO_2} \Delta\alpha_i}{\sum_i S_{iSO_2} \Delta\alpha_i}. \quad (4)$$


**Fig. 2.** Panoramic view of the oil refinery and the Montevideo Bay from the measuring site. The dashed rectangle indicates the emitting stack group. The cross scanned sections are numbered from 1 to 6.

For the sake of simplicity, in the following we will consider that the $SO_2$- and the $NO_x$-flux are constant during the time interval (minutes, see above) necessary for the measurements.

Then, comparing the measurements at two different cross sections of the plume, denoted as cross section 1 and cross section 2, from Eq. (4) it is possible to estimate the $NO_2$-formation rate (molec $s^{-1}$ or equivalent) in the volume between the cross sections:

$$\frac{dn_{NO_2}}{dt} = \Phi_{NO_2}\big|_2 - \Phi_{NO_2}\big|_1 = \Phi_{SO_2}\left[\left.\frac{\sum_i S_{iNO_2}\Delta\alpha_i}{\sum_i S_{iSO_2}\Delta\alpha_i}\right|_2 - \left.\frac{\sum_i S_{iNO_2}\Delta\alpha_i}{\sum_i S_{iSO_2}\Delta\alpha_i}\right|_1\right], \quad (5)$$

where $n_{NO_2}$ is the number of $NO_2$-molecules (or equivalent), and the subscripts 1 and 2 denote the cross section 1 and cross section 2, respectively.

Equations (4) and (5) can be simplified by introducing mean slant column densities defined as

$$\bar{S}_{NO_2,SO_2} \equiv \frac{\sum_i S_{iNO_2,SO_2}\Delta\alpha_i}{\sum_i \Delta\alpha_i} \quad (6)$$

where the index $i$ runs through the slant column densities measured across the plume.

Substituting Eq. (6) into (4), one obtains

$$\Phi_{NO_2} = \Phi_{SO_2}\frac{\bar{S}_{NO_2}}{\bar{S}_{SO_2}}, \quad (7)$$

and then, from Eq. (5) it finally results

$$\frac{dn_{NO_2}}{dt} = \Phi_{SO_2}\left[\left(\frac{\bar{S}_{NO_2}}{\bar{S}_{SO_2}}\right)_2 - \left(\frac{\bar{S}_{NO_2}}{\bar{S}_{SO_2}}\right)_1\right]. \quad (8)$$

This expression tells us that, under the assumption that $\Phi_{SO_2}$ is known (and constant), one can obtain the $NO_2$-formation rate ($dn_{NO_2}/dt$) alone from the measurement of slant column densities without explicit knowledge of the wind velocity and distance to the plume. In fact, the plume may be changing its shape, i.e. the wind may change its speed and direction between consecutive cross-scans. Even more, the distance between the measuring site and the plume ($R$) may be changing in time, e.g. the observation site may be in movement between consecutive cross-scans. Note, however, that the wind velocity inside the plume could actually be measured by correlation techniques (Galle et al., 2010), but this was not attempted in our study.

Actually, since we are assuming that the geometrical cross section of the plume is small in comparison with the distance to the observation site, we can consider that the range of elevation angles in which the slant column densities have significant values is relatively narrow. Thus, as a first approximation, in Eqs. (7) and (8) the mean values $\bar{S}_{NO_2,SO_2}$ could be calculated by considering only the slant column densities restricted to an interval of elevation angles, where the slant column densities are significantly higher than the background.

As discussed in detail below, for the separation of the plume from a possible background, it is important that the elevation scans cover the full plume.

## 3 Test measurements at Montevideo

### 3.1 Measurement procedure

In order to validate our proposal, we performed some test measurements of emissions from a petrochemical facility, located in the north of the Montevideo Bay (34.5° S, 56.1° W). The measurements were made in the period February–March 2011.

The refinery has many stacks and there is no public information about its emissions. For the flux estimation, we simplify the analysis by assuming a single emitter and use the slant column density data downwind after the last stack of the group.

The measurements were performed from the west side of the Bay, approximately 1.9 km away from the stacks of the refinery. From this place, we were able to perform vertical scans of the plume at different distances from the source. Also, from this place it was easy to find reference points in the city (e.g. telecommunication building, etc.) which allow

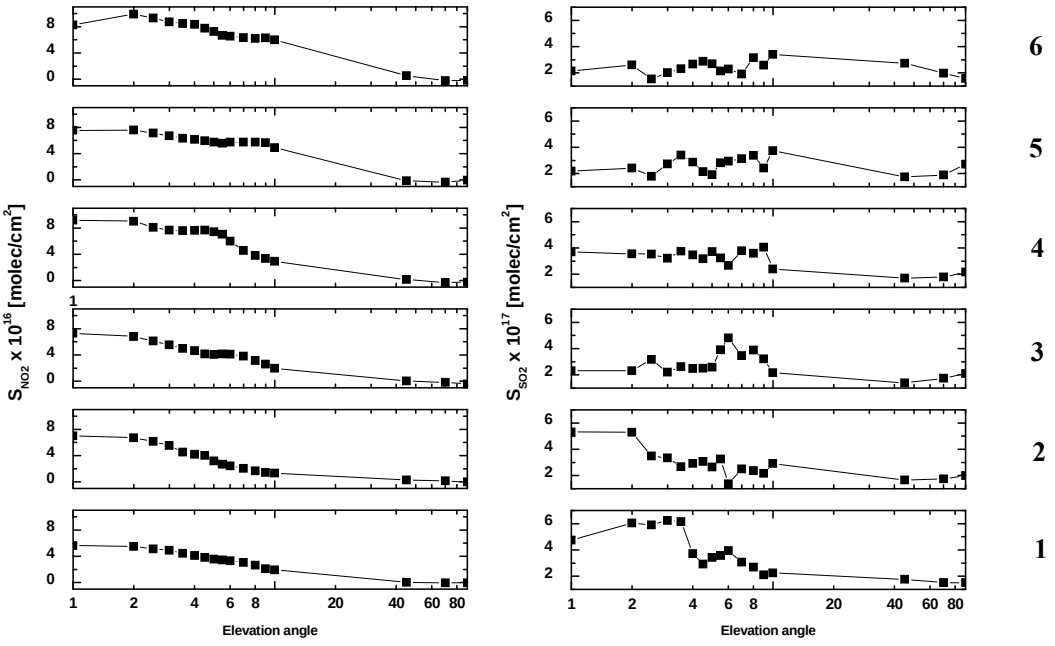


**Fig. 3.** $NO_2$ and $SO_2$ slant column densities by vertical scans 1 to 6 and elevation angles 1° to 90° (please notice the logarithmic scale for the elevation angles).

evaluating the length of the distance traversed by the plume. A panoramic picture of the site is shown in Fig. 2 (the dotted rectangle indicates the location of the main stack group).

A miniaturized Multi Axis – Differential Optical Absorption Spectroscopic (MAX-DOAS) instrument with an instantaneous field of view of 0.4°, spectral range of 311–460 nm and spectral resolution of ∼0.44–0.75 nm was used. A detailed description of the instrument is in Bobrowski et al. (2006) (see also Hönninger, 2004; Frins et al., 2011). The vertical scans were performed in the range from 0°–10° in steps of 0.5°–1°. In addition, elevation angles of 45°, 70° and 90° were also measured.

After a quick evaluation in place, it was found that the significantly enhanced trace gases concentrations were probably in the range of elevation angles 0°–10°. For viewing directions outside this range the $SO_2$-SCD was typically of the order of $2 \times 10^{17}$ molec cm$^{-2}$ (see Fig. 3), which is close to our detection limit (∼0.5–1 $\times 10^{17}$ molec cm$^{-2}$).

In our study, $NO_2$- and $SO_2$-slant column densities were evaluated in the spectral ranges 430–460 nm and 315–325 nm respectively. A zenith spectrum collected at midday of the same day was used as reference, and the slant column densities were computed using the WINDOAS software (Fayt and Van Roozendael, 2001), which implements the spectral analysis via a minimization algorithm.

For the $NO_2$ evaluation, the absorption cross sections of $O_4$ (Greenblatt et al., 1990) and $NO_2$ (Vandaele et al., 1998) at 294 K, $O_3$ (Burrows et al., 1999) at 294 K and water vapor at 290 K (Rothman et al., 2005) were utilized. Additionally a synthetic Ring spectrum was included in the evaluation (Wagner et al., 2009).

For the $SO_2$ analysis, absorption cross sections of $SO_2$ at 294 K (Vandaele et al., 1994), $O_3$ at 294 K (Burrows et al., 1999) and a synthetic Ring spectrum were included (Wagner et al., 2009). Since the literature cross sections are given in cm$^2$ molecule$^{-1}$ we obtain column densities in molecules cm$^{-2}$ and concentrations in molecules cm$^{-3}$. These concentrations were converted to kg m$^{-3}$ using the known molar mass of the species.

We used wind data provided by a portable weather station located at our site and by Melilla Airport at 10 km north from our measuring site. Actually, we need the wind data only for the purpose of determining the $SO_2$-flux, but this flux could eventually be known through other methods (e.g. in-stack monitors or fuel-consum mass-balance).

### 3.2 Experimental results

On 29 March 2011 we performed measurements across six vertical cross sections (numbered from 1 to 6, 3–4 min each single vertical scan) of the plume emitted by the oil refinery (see Fig. 2). We chose a sunny day with good meteorological conditions (a quite clear ambient atmosphere, free from clouds or aerosols). The plume was transparent and we did not observe any scattering inside the plume, thus we conclude that there was negligible aerosol scattering. We estimated the visibility range at about 30 km, corresponding to an aerosol scattering coefficient of about 0.13 km$^{-1}$. At an estimated plume width (along the line of DOAS observation)

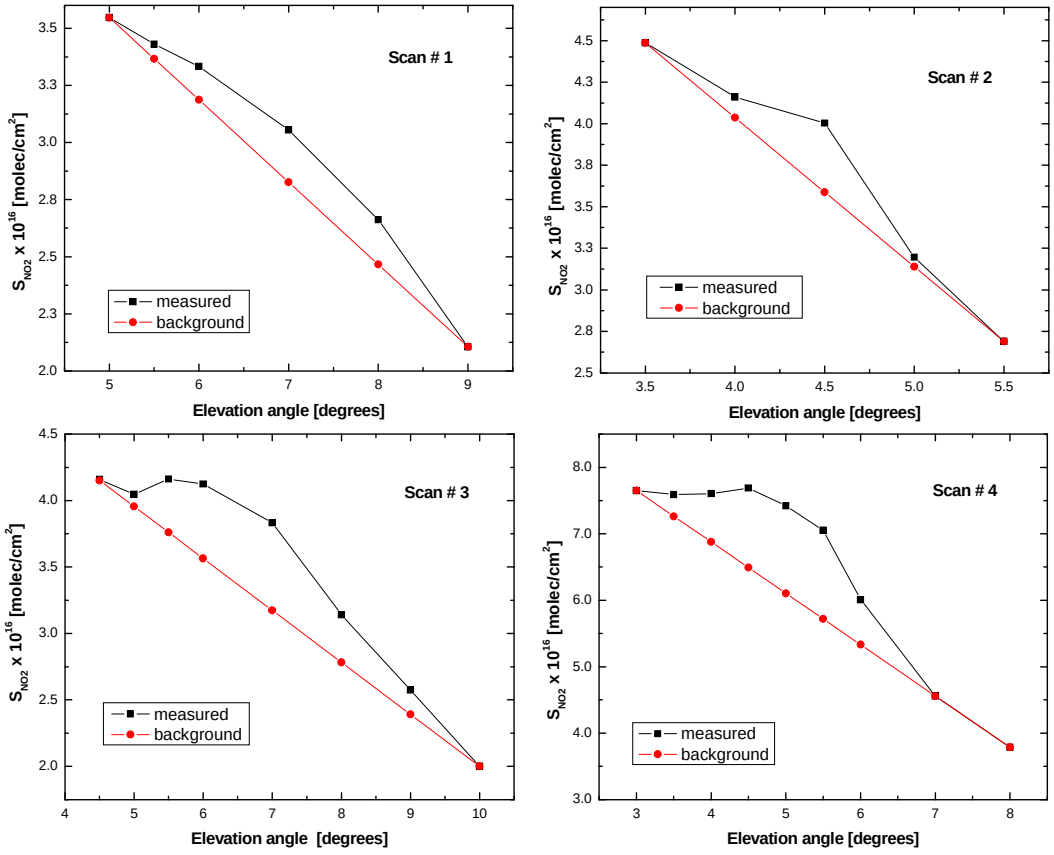


**Fig. 4.** Illustration of the estimation of the lower limit for the contribution of the emission plume to the measured $NO_2$ SCDs for scans #1–4. It is assumed that the possible contribution from the background causes a smooth variaion of the SCDs (approximated) by the red line. The difference of the measured SCDs to the red line is attributed to the emission plume (Note that for scan 1 the contribution from the emission plume is probably even smaller, because the smooth variation of the SCDs can in principle be explained by the presence of a tropospheric background alone).

of 0.2 km this would correspond to a scattering probability of about 0.03 within the plume, and thus, clearly multiple scattering will be negligible under these conditions. The virtual absence of multiple scattering was also confirmed by the evaluation of $O_4$.

We used a cross scan near the stacks to quantify the flux $\Phi_{SO_2}$. During the measurements across section 1, the mean wind velocity was $\sim$6.4 km h$^{-1}$ blowing from NNE. Using the measured $SO_2$-SCDs as function of the elevation angle in Eq. (2), we obtained a $SO_2$-flux of the order of 300 kg h$^{-1}$ $\pm$ 120 kg h$^{-1}$.

The uncertainty estimation of the SCD values measured in this work is based on the errors determined by the numerical fitting, depending on the size and structure of the residual. The estimated uncertainties (see Stutz and Platt, 1997) of the SCDs were of the order of 30 % and 10 % for $SO_2$ and $NO_2$, respectively. The uncertainty of the wind speed was about 30 % (due to changes of the wind speed and direction). Thus, it results an uncertainty in the fluxes of the order of 40 %. As discussed below, for the estimation of the $NO_2$ flux, additional uncertainties arise from the contribution of a possible tropospheric background concentration.

In our case the distance to the plume was of the order of 2 km, and thus, no significant radiation dilution effects are to be expected (Kern et al., 2009).

During the measurements across sections 1–6 the wind was changing in speed (6.4–12.9 km h$^{-1}$ corresponding to 1.8–3.6 m s$^{-1}$) and direction (NNE to NNW), but we will assume that the $SO_2$- and $NO_x$-flux emitted by the refinery remains constant in the short time interval (20 min) required for the measurements.

Figure 3 shows the obtained $SO_2$- and $NO_2$-slant column densities at the different cross sections at elevation angles between 1° and 90°.

For scans 1–4, the measured trace gas SCDs decrease when elevation angles increase from 1° to 10°. For elevation angles >10°, the measured SCDs are typically even lower and close to the detection limit. In contrast, for scans 5 and 6, the SCDs at 10° elevation show no clear decrease indicating that probably the emission plume is not fully covered

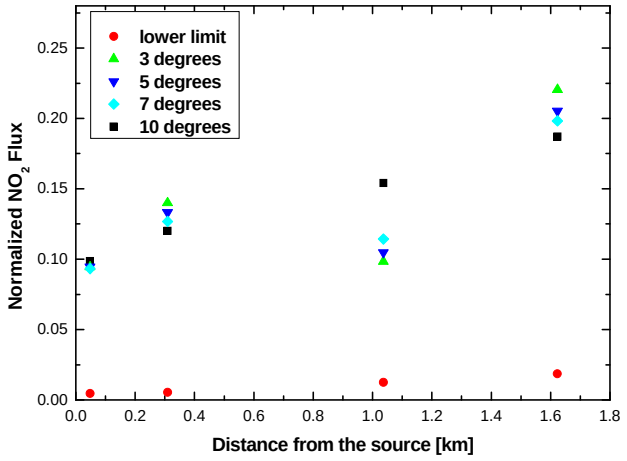


**Fig. 5.** Normalized $NO_2$-fluxes $\bar{S}_{NO_2}/\bar{S}_{SO_2}$ (after Eq. 7); the mean values $\bar{S}_{NO_2,SO_2}$ were calculated by considering the slant column densities restricted to different intervals of elevation angles (3°, 5°, and 7°) and the whole range 1°–10°. The result for the lower limit (see Fig. 4) is also presented.

by elevation angles $\leq$10°. Thus we skip these scans in the further analysis.

Another limitation is found for the $NO_2$ SCDs: while for $SO_2$, the highest SCDs (in scans 1–3) occur at different elevation angles (probably indicating that the plume is affected by turbulent transport), for $NO_2$, the dependence of the SCDs on elevation angles shows a rather smooth behaviour. Thus for $NO_2$ we can not rule out that a substantial part of the measured SCDs might be caused by a tropospheric background (caused by the emissions from the city) and not by the emission plume. Moreover, since we have to assume that such a background contribution might vary with space and time, there is no simple way to quantify and subtract it from our MAX-DOAS measurements.

One conclusion from these findings is to improve the measurement strategies for future measurements. In particular, more observations should be performed to determine a possible background contribution and to separate it from the emission plume of interest. For that purpose we suggest the following strategies:

a. The full plume should be covered with moderate distance between elevation angle. This will allow to identify the emission plume by its specific shape.

b. Emission plumes should be scanned from closer locations. This will cause higher elevation angles under which the plume will be seen. Under such angles, a possible background contribution will be smaller and can be better separated from the emission plume.

c. The sequence of scans at different azimuth angles should be repeated to quantify the temporal variability of both the emission plume and the background concentration.

d. The first elevation scan should be performed upwind of the emission source.

Unfortunately, for our measurements, we can not apply similar strategies to separate the contributions from plume and background due to the lack of observations. Instead we used the existing observations and determine an upper and lower limit for the contribution of the plume to the measured SCD:

– To determine an upper limit, we simply assume that the measured $NO_2$ SCDs (below 10° elevation) are entirely caused by the emission source.

– To determine the lower limit, we only assign the part of the measured $NO_2$ SCDs to the emission source, which can not be explained by a tropospheric background due to the specific dependence of the SCDs on elevation angle. This method is illustrated in Fig. 4.

Figure 5 shows these upper and lower limits of the normalized $NO_2$-fluxes $\bar{S}_{NO_2}/\bar{S}_{SO_2}$ (i.e., the $NO_2$-fluxes normalized with $\Phi_{SO_2}$) as function of the distance to the source. For illustrative purposes, the mean values $\bar{S}_{NO_2,SO_2}$ of the upper limits were calculated by considering the slant column densities restricted to different intervals of elevation angles (e.g. 3°, 5°, and 7°), and also for the whole range 1°–10°. Although there is an increased dispersion of the $\bar{S}_{NO_2}/\bar{S}_{SO_2}$ values when the mean values $\bar{S}_{NO_2,SO_2}$ are calculated by considering small intervals of elevation angles, Fig. 5 shows clearly an increase of the $NO_2$-flux with the distance to the source.

Also, the lower limits show an increase with distance from the source. However, as has to be expected, the absolute values are much lower.

A linear fit of the results obtained in the interval 1°–10° tells us that the $NO_2$-formation rate per unit distance is of the order of 16 ($\pm$11) kg h$^{-1}$ km$^{-1}$, assuming a $SO_2$-flux of 300 kg h$^{-1}$. The $NO_2$-formation rate per unit length considering 3° interval of elevation angles is 18 ($\pm$12) kg h$^{-1}$ km$^{-1}$, and 16 ($\pm$11) kg h$^{-1}$ km$^{-1}$ for 5° and 7° interval of elevation angles.

Following the procedure describe in Fig. 5 the obtained lower limit of the formation rate of $NO_2$ is of the order of 3 ($\pm$ 2) kg h$^{-1}$ km$^{-1}$. Upper and lower limits of the $NO_2$-formation rate per unit distance was calculated as the product of $\Phi_{SO_2}$ and the slope of the linear fit (slope $\approx$0.054 km$^{-1}$; correlation coefficient $\approx$0.99 for the upper limit and slope $\approx$0.010 km$^{-1}$; correlation coefficient $\approx$0.99 for the lower limit).

## 4 Conclusions

In the present paper we deal with gaseous emissions originating from combustion processes containing $SO_2$ and $NO_x$, emitted into the atmosphere by a localized source. We presented a method for measuring the $NO_2$-formation rate (due to conversion of NO to $NO_2$) from measurements of mean $SO_2$- and $NO_2$-slant column densities across different plume sections. The proposed method is based on the assumption that the $SO_2$- and $NO_x$-flux emitted by the source remains constant during the measuring time.

The advantage of the proposed method is that explicit knowledge of the wind speed and direction across the different plume sections is not required. Actually, the wind may change its speed and direction between consecutive plume cross-section scans, and/or the distance to the plume ($R$) may be changing in time, e.g. the observation site may be in motion, as long as the line of sight traverses the entire plume section.

We present results of ground based measurements of $SO_2$ and $NO_2$ from the emissions of an oil refinery located in the northern part of Montevideo Bay. We derive a $SO_2$ flux of $300\,kg\,h^{-1}$ and a $NO_2$ formation of 16 ($\pm$11) $kg\,h^{-1}\,km^{-1}$. The rather large uncertainties for the $NO_2$ fluxes are related to difficulties in separating the contribution from the emission plume from a possible tropospheric background. We give recommendations for future applications of our method to minimise such interference.

*Acknowledgements.* This work was supported by the Comisión Sectorial de Investigación Científica (CSIC) of the Universidad de la República (Uruguay), PEDECIBA (Programa de Apoyo a las Ciencias Básicas) and ANII (Agencia Nacional de Investigación e Innovación) contract number ANII-PR-FSE-2009-1-26. The authors thank Ossama Ibrahim and Federico Arismendi for their assistance during the measurements performed on December 2009.

Edited by: K. Kreher

## References

Bobrowski, N. and Platt, U.: $SO_2$/BrO ratios studied in five volcanic plumes, J. Volcanol. Geoth. Res., 166, 147–160, doi:10.1016/j.jvolgeores.2007.07.003, 2007.

Bobrowski, N., Hönninger, G., Lohberberg, F., and Platt, U.: IDOAS: A new monitoring technique to study the 2D distribution of volcanic gas emissions, J. Volcanol. Geoth. Res., 150, 329–338, doi:10.1016/j.jvolgeores.2005.05.004, 2006.

Burrows, J. P., Dehn, A., Deters, B., Himmelmann, S., Richter, A., Voigt, S., and Orphal, J.: Atmospheric Remote-Sensing Reference Data from GOME: 2, Temperature-Dependent Absorption Cross Sections of $O_3$ in the 231–794 nm Range, J. Quant. Spectrosc. Ra., 61, 509–517, doi:10.1016/S0022-4073(98)00037-5, 1999.

Fayt, C. and van Roozendael, M.: WinDOAS 2.1, Software User Manual, Belgian Institute for Space Aeronomy, Brussels, Belgium, available at: http://bro.aeronomie.be/WinDOAS-SUM-210b.pdf (last access: 17 May 2012), 2001.

Frins, E., Bobrowski, N., Platt, U., and Wagner, T.: Tomographic multiaxis-differential optical absorption spectroscopy observations of Sun-illuminated targets: a technique providing well-defined absorption paths in the boundary layer, Appl. Optics, 45, 6227–6240, 2006.

Frins, E., Ibrahim, O., Casaballe, N., Osorio, M., Arismendi, F., Wagner, T., and Platt, U.: Ground based measurements of $SO_2$ and $NO_2$ emissions from the oil refinery "La Teja" in Montevideo city, J. Phys. Conf. Ser., 274, 012083, doi:10.1088/1742-6596/274/1/012083, 2011.

Galle, B., Johansson, M., Rivera, C., Zhang, Y., Kihlman, M., Kern, C., Lehmann, T., Platt, U., Arellano, S., and Hidalgo, S.: Network for Observation of Volcanic and Atmospheric Change (NOVAC) – A global network for volcanic gas monitoring: Network layout and instrument description, J. Geophys. Res., 115, D05304, doi:10.1029/2009JD011823, 2010.

Greenblatt, G. D., Orlando, J. J., Burkholder, J. B., and Ravishankara, A. R.: Absorption Measurements of Oxygen between 330 and 1140 nm, J. Geophys. Res., 95, 18577–18582, doi:10.1029/JD095iD11p18577, 1990.

Hönninger, G.: Ground-based measurements of halogen oxides at the Hudson Bay by active longpath DOAS and passive MAX-DOAS, Geophys. Res. Lett., 31, L04111, doi:10.1029/2003GL018982, 2004.

Kern, Ch., Deutschmann, T., Vogel, L., Wöhrbach, M., Wagner, Th., and Platt, U.: Radiative transfer corrections for accurate spectroscopic measurements of volcanic gas emissions, B. Volcanol., 72, 233–247, doi:10.1007/s00445-009-0313-7, 2009.

Lee, C., Martin, R. V., van Donkelaar, A., Lee, H., Dickerson, R. R., Hains, J. C., Krotkov, N., Richter, A., Vinnikov, K., and Schwab, J. J.: $SO_2$ emissions and lifetimes: Estimates from inverse modeling using in situ and global, space-based (SCIAMACHY and OMI) observations, J. Geophys. Res., 116, D06304, doi:10.1029/2010JD014758, 2011.

Louban, I., Bobrowski, N., Rouwet, D., Inguaggiato, S., and Platt, U.: Imaging DOAS for volcanological applications, B. Volcanol., 71, 753–765, doi:10.1007/s00445-008-0262-6, 2009.

McGonigle, A. J. S., Thomson, C. L., Tsanev, V. I., and Oppenheimer, C.: A simple technique for measuring power station $SO_2$ and $NO_2$ emissions, Atmos. Environm., 38, 21–25, doi:10.1016/j.atmosenv.2003.09.048, 2004.

Platt, U. and Stutz, J.: Differential Optical Absorption Spectroscopy: Principles and Applications, Heidelberg: Springer Verlag, 2008.

Rivera, C., Mellqvist, J., Samuelsson, J., Lefer, B., Alvarez, S., and Patel, M. R.: Quantification of $NO_2$ and $SO_2$ emissions from the Houston Ship Channel and Texas City industrial areas during the 2006 Texas Air Quality Study, J. Geophys. Res., 115, D08301, doi:10.1029/2009JD012675, 2010.

Rothman, L. S., Jacquemart, D., Barbe, A., Benner, D. C., Birk, M., Brown, L. R., Carleer, M. R., Chackerian Jr., C., Chance, K., Coudert, L. H., Dana, V., Devi, V. M., Flaud, J.-M., Gamache, R. R., Goldman, A., Hartmann, J.-M., Jucks, K. W., Maki, A. G., Mandin, J.-Y., Massie, S. T., Orphal, J., Perrin, A., Rinsland, C. P., Smith, M. A. H., Tennyson, J., Tolchenov, R. N., Toth, R. A.,

Vander Auwera, J., Varanasi, P., and Wagner, G.: The HITRAN 2004 molecular spectroscopic database, J. Quant. Spectrosc. Ra., 96, 139–204, doi:10.1016/j.jqsrt.2004.10.008, 2005.

Seinfeld, J. and Pandis, S.: Atmospheric Chemistry and Physics: From Air Pollution to Climate Change, Wiley-Interscience, 2006.

Stutz, J. and Platt, U.: Numerical analysis and estimation of the statistical error of differential Optical absorption spectroscopy measurements with least-squares methods, Appl. Optics, 35, 6041–6053, doi:10.1364/AO.35.006041, 1997.

Vandaele, A. C., Simon, T. C., Goilmont, J. M., Carleer, C. M., and Colin, R.: $SO_2$ absorption cross section measurement in the UV using a Fourier tranform spectrometer, J. Geophys. Res., 99, 25599–25605, doi:10.1029/94JD02187, 1994.

Vandaele, A. C., Hermans, C., Simon, P. C., Carleer, M., Colins, R., Fally, S., Mérienne, M. F., Jenouvrier, A., and Coquart, B.: Measurements of the $NO_2$ absorption cross-sections from 42 000 $cm^{-1}$ to 10 000 $cm^{-1}$ (238–1000 nm) at 220 K and 294 K, J. Quant. Spectrosc. Ra., 59, 171–184, doi:10.1016/S0022-4073(97)00168-4, 1998.

Wagner, T., Beirle, S., and Deutschmann, T.: Three-dimensional simulation of the Ring effect in observations of scattered sun light using Monte Carlo radiative transfer models, Atmos. Meas. Tech., 2, 113–124, doi:10.5194/amt-2-113-2009, 2009.

Weibring, P., Edner, H., and Svanberg, S.: Versatile mobile Lidar system for environmental monitoring, Appl. Optics, 42, 3583–3594, doi:10.1364/AO.42.003583, 2003.